

L-shell x-ray cross sections for Cl-Ar and Ar-Ar collisions

H. Oona and J. D. Garcia

Department of Physics, University of Arizona, Tucson, Arizona 85721

R. J. Fortner

Lawrence Livermore Laboratory, Livermore, California 94550

(Received 15 April 1977)

Measurements of total x-ray production cross sections for Ar⁺-Ar and Cl⁺-Ar collisions for incident energies between 200 keV and 1.5 MeV are reported. For Cl⁺-Ar collisions, separate argon and chlorine x-ray production cross sections are extracted. The cross sections exhibit steep increases as bombarding energy is increased. Using existing measurements of Auger cross sections, values for the mean fluorescence yields as a function of bombarding energy are deduced. The increases in the x-ray production cross sections are shown to be due primarily to changes in the mean fluorescence yields. A qualitative explanation for the observations is proposed.

I. INTRODUCTION

Atomic *L*-shell excitation mechanisms and the accompanying relaxation processes are considerably more complicated than the corresponding events associated with the *K* shell. The angular momentum associated with the *L*-shell vacancy results in a large increase in the number of initial states possible in a multiply ionized atom. The concomitant richness of available states, as well as smaller binding energies, produces a plethora of possibilities which at first glance would seem prohibitive. It is nevertheless true that *L*-shell excitation of the Ar atom in Ar-Ar collisions^{1,2} provided the basis for our current understanding of excitation mechanisms in ion-atom collisions in terms of the quasimolecule formed during the collision.³⁻⁶ The applicability of molecular orbitals to ion-atom collisions reduces the complexity of the excitation processes to a quantitatively tractable problem,^{7,8} as well as providing the necessary link between the various manifestations of an inner-shell excitation; e.g., Auger electron emission, x-ray emission, and inelastic energy losses.^{5,6}

Several systematic studies⁹⁻¹¹ of *L*-shell excitation in both homonuclear and heteronuclear ion-atom collisions have yielded substantial progress in our understanding of both the excitation processes and the decay mechanisms for the *L* shell. Quantitative calculations for the two dominant excitations, the $4f\sigma$ promotion¹² and the $3d\sigma$ promotion,¹³ are in reasonable accord with experiment. It is now evident, in addition, that the aforementioned richness of states plays a substantial role in the deexcitation processes. That this too is amenable to quantitative analysis is brought out by analysis of fluorescence yield calculations.¹⁴

Most of the studies to date have been concentrated on collision energies less than 200 keV. In this

paper we investigate Cl-Ar and Ar-Ar collisions in the 200–1500-keV energy range. We have experimentally determined the x-ray emission cross sections for both chlorine and argon *L* shells in this energy range. These data are then used in conjunction with evidence from other *L*-shell excitation signatures to provide values for the respective mean fluorescence yields, as functions of the collision energy. The x-ray emission cross sections show a rapid increase with increasing energy, with a tendency to level off at the highest energies. The dependence of the *L*-shell x-ray emission cross section on projectile atomic number is found to decrease at higher projectile energies. Most of these changes are attributable to changes in the fluorescence yields.

II. EXPERIMENTAL PROCEDURE

This experiment was performed using the University of Arizona's 2-MeV Van de Graaff accelerator. The measurements were performed using a high-resolution (Norelco) bent-crystal x-ray spectrometer with a lead stearate crystal. The detector was a flow-mode proportional counter with a nominally 2000-Å-thick parylene window. The target consisted of a gas cell containing He-isobutane gas at a pressure of 5×10^{-2} Torr. The beam entered through a 1-mm aperture and the x rays were observed at 90° with respect to the beam direction through a 2000-Å-thick parylene window. The importance of using thin windows for chlorine and Ar *L*-shell x-ray experiments has been demonstrated elsewhere.¹¹ The resolution of the system was about 1.5 eV for 200-eV photons. Spectra were taken at different bombarding energies from 200 keV to 1.5 MeV for a fixed amount of beam.

The total relative intensity was obtained by integrating the spectra after correcting for crystal

reflectivity¹⁵ and window transmission.¹⁶ (See Figs. 1 and 2 of Ref. 11.) Care must be taken in performing this integration. The yield per incident ion in a given spectral interval ΔE_ν at E_ν is related to the differential cross section by

$$Y_x(E_\nu) = \frac{d\sigma_x}{dE_\nu} \left(\epsilon T I P l \frac{\Delta\Omega}{4\pi} \right) \Delta E_\nu, \quad (1)$$

where ϵ is the counter efficiency, T the transmission of the windows, I the ion current, P the pressure in the target cell, l the observed path length, and $\Delta\Omega$ the effective solid angle. If the spectrometer is operated such that $\Delta\theta_B$, the observed Bragg angle interval is held constant, and $\Delta\Omega$ does not change,

$$\frac{d\sigma_x}{dE_\nu} = \frac{1}{Z} \frac{Y_x(E_\nu)}{dE_\nu/d\theta_B}, \quad (2)$$

where $Z = \epsilon T I P l \Delta\theta_B$, and, using fixed intervals ΔE_ν in the integration,

$$\sigma_x = \int \frac{d\sigma_x}{dE_\nu} dE_\nu = \frac{\Delta E_\nu}{Z} \sum_i \frac{Y_x[E_\nu(i)]}{|dE_\nu/d\theta_B|_i}. \quad (3)$$

Here of course $dE_\nu/d\theta_B$ is given by the Bragg relation

$$\left| \frac{dE_\nu}{d\theta_B} \right| = \frac{2E_\nu^2 d}{hc} \left[1 - \left(\frac{hc}{2E_\nu d} \right)^2 \right]^{1/2},$$

where h is Planck's constant, c the speed of light, and d the crystal lattice spacing ($2d = 100.688 \text{ \AA}$ for lead stearate crystals). If, instead, the spectrometer is designed such that $\Delta\lambda/\lambda (= |\Delta E_\nu/E_\nu|)$ is held constant, the weighting in Eq. (3) would be different. This discussion is valid only if (as is usually the case) the instrumental resolution is much larger than the natural width. In our experiment, as will be seen below, the integrals in (3) are dominated by one or two adjacent spectral features and the effect of this weighting (conversion from constant angular increments to energy increments) is minimized.

The total x-ray emission cross sections in these experiments were determined by normalizing the observed total relative intensities to the known L -shell x-ray cross section for Cl-Ar and Ar-Ar collisions at 200 keV.¹¹ The normalization factor was actually determined from the Ar-Ar total x-ray intensities. It was found that the same normalization factor also properly normalized the total Cl-Ar intensity at 200 keV.

III. ANALYSIS OF THE DATA

Figure 1 shows typical spectra for $\text{Cl}^+\text{-Ar}$, $\text{Cl}^+\text{-Cl}_2$, and $\text{Ar}^+\text{-Ar}$ collisions at 500 keV, 1 MeV, and 1 MeV, respectively.¹⁷ Though the resolution is insufficient to observe individual multiplet structure,

the gross features in the spectra can be interpreted using adiabatic Hartree-Fock calculations.^{11, 18} For example, in the $\text{Cl}^+\text{-Cl}_2$ data the features below 210 eV correspond to emissions by atoms with one L -shell vacancy and various numbers of M -shell vacancies. The features from 210 eV to about 250 eV correspond to emissions by atoms with two L -shell vacancies and varying numbers of M -shell vacancies. The structure above 255 eV is attributed to atoms with three L -shell vacancies and various M -shell configurations. Similar identifications for the structures in the other two spectra can be found. Actually these interpretations are an oversimplification of the actual situation. As indicated in Ref. 18, the spread in energy of x rays associated with a given configuration can be as large as 20 eV or more, due to multiplet structure. However, this does not in general change the conclusions arrived at from configuration centroid identifications because many of the components are quite weak. In any case, no complete detailed accurate theoretical analysis is available for all of the possible configurations, and the experimental resolution is not sufficient to provide an ambiguous identification in most cases.

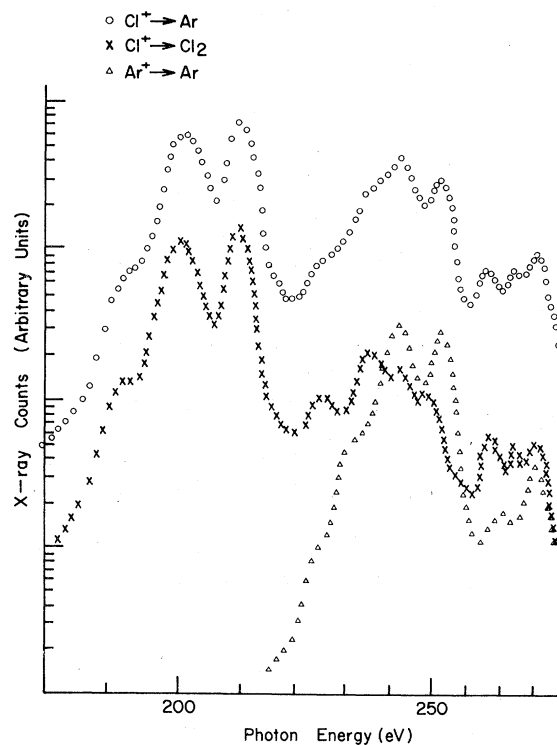


FIG. 1. Spectra from $\text{Cl}^+\text{-Ar}$ (500 keV), $\text{Cl}^+\text{-Cl}_2$ (1 MeV), and $\text{Ar}^+\text{-Ar}$ (1 MeV) collisions. The open circles show the $\text{Cl}^+\text{-Ar}$ data, the crosses depict the $\text{Cl}^+\text{-Cl}_2$ data and the open triangles show the $\text{Ar}^+\text{-Ar}$ data, as functions of the photon energy.

Despite the above-mentioned difficulties, most major features in all three spectra can be easily identified. These identifications are based on the fact that the majority of the L -shell vacancy states have fluorescence yields which are quite small (i.e., 10^{-4} – 10^{-2}), whereas, when the M shell is nearly emptied, there are states which have *unit* fluorescence yields. In the Cl^+-Cl_2 spectrum, for example, the peak at 210 eV coincides in energy with well known $2p^6-2p^53s$ transitions,¹⁹ with $\omega=1$. Similarly, the peaks at 236, 241, and 253 eV are associated with known $2p^5-2p^43s$ transitions.¹⁹ The peaks at 268, 272, and 280 eV can likewise be related to $2p^3-2p^23s$ transitions.¹⁹ In contrast, the peaks at 200 eV, 225 eV, and part of the peak at 268 eV appear to be due to transitions involving one, two, and three L -shell vacancies, respectively, with more than one M -shell electron present.

An entirely analogous spectral analysis of the Ar^+-Ar peaks is possible. The peaks at 253 and 280 eV correspond to $2p^5-2p^53s$ and $2p^5-2p^43s$ transitions, respectively,¹⁹ while those at 240 and 270 eV again correspond to transitions with one and two L -shell vacancies with more M -shell electrons present. The Cl^+-Ar spectrum appears to be a simple composite of the chlorine and argon spectra.

Fortunately, for purposes of this paper, only minimal understanding of the spectral features is necessary. First of all, no interpretation of the Ar^+-Ar spectra is necessary. The observed spectra at each bombarding energy are simply integrated to yield a relative x-ray emission cross section. These relative cross sections are converted into absolute cross sections by the normalization procedure described in Sec. II.

Some consideration of the instrumental cutoff at 284 eV (the carbon K absorption edge) is, however, necessary. Argon atoms with more than one L -shell vacancy can emit x rays whose energies lie above this edge. However, as discussed in Ref. 11, the fluorescence yields associated with L -shell vacancies, and the decay schemes of such atoms are such that the contributions to the total x-ray yield are dominated by single L -shell vacancy configurations. This can be seen to be the case in the Cl^+-Cl_2 spectrum in Fig. 1. The reason for this is that the Auger effect is the dominant relaxation process for L shells. Thus, atoms with two L -shell vacancies predominantly decay by filling one vacancy from the M shell while simultaneously ejecting another M -shell electron. The resultant single vacancy configuration has two additional M -shell vacancies. Such configurations have fluorescence yields which are very much larger¹⁴ than those for the original state. This results finally in predominance of the x-ray spectrum by the high fluores-

cence yield single vacancy x rays.

The total x-ray emission cross sections for Cl^+-Ar collisions similarly need no interpretation. The fact that the chlorine and argon single L -shell vacancy spectral features are well separated in energy provides the basis for the separation of the argon and chlorine contributions to the total Cl^+-Ar cross sections. As described in Refs. 11 and 17, experimentally determined Cl^+-Cl_2 and Ar^+-Ar spectra are superimposed to reproduce the Cl^+-Ar spectrum. The relative intensities associated with each are then converted into cross sections.

We estimate, on the basis of the above considerations, that the uncertainties in our total x-ray emission cross sections are about 50% and probably no more than a factor of 2 for the Ar cross sections in Cl^+-Ar collisions.

Figure 2 shows the resultant cross sections as a function of bombarding energy. For completeness, we have included all the L -shell x-ray emission cross section measurements which are available, including lower-energy collisions. These addition-

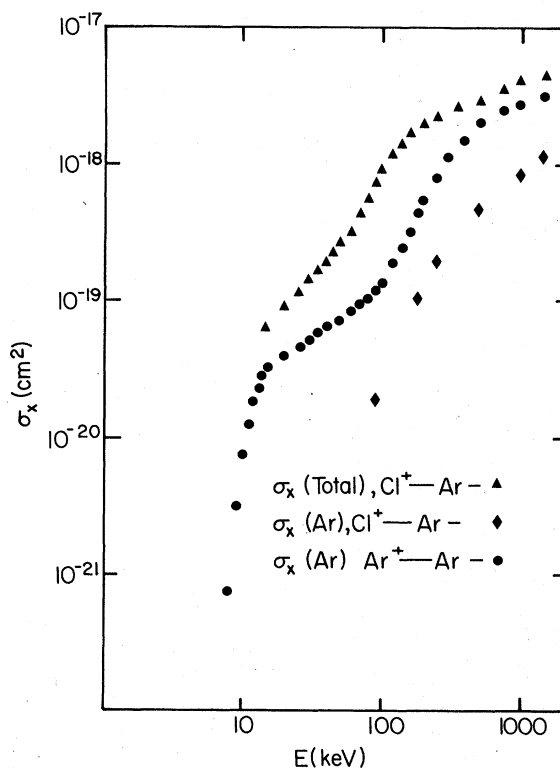


FIG. 2. X-ray emission cross sections for Cl^+-Ar and Ar^+-Ar collisions as a function of bombarding energy. The triangles show the total Cl^+-Ar cross sections. The diamonds indicate the Ar x-ray emission cross section for Cl^+-Ar collisions, and the circles show the total Ar^+-Ar cross sections. The data below 200 keV are from Refs. 9 and 11.

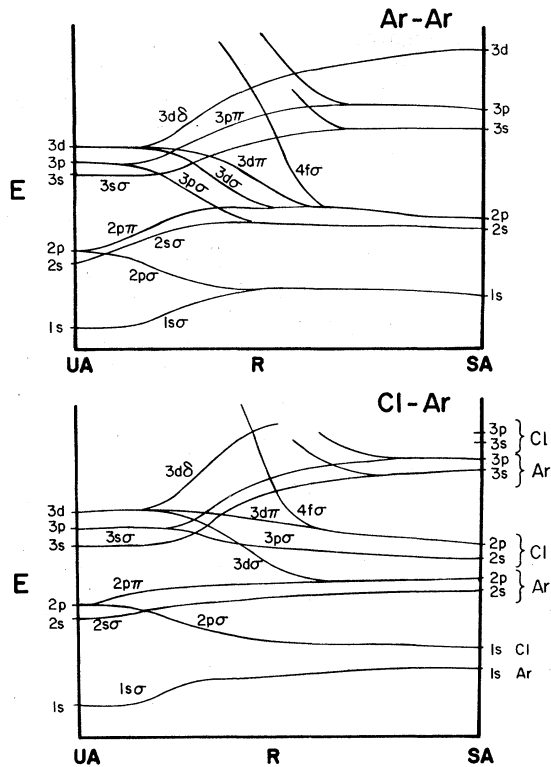


FIG. 3. Schematic correlation diagrams for Ar-Ar and Cl-Ar molecules. The left-hand side depicts the united atom limit and the right-hand side corresponds to the separated atom limit.

al cross sections came from the following sources: for Ar^+ -Ar collisions below 25 keV, Ref. 9 (these were normalized to those in Ref. 11); for Ar^+ -Ar collisions between 25 and 200 keV, Ref. 11; for Cl^+ -Ar collisions below 200 keV, Ref. 11.

For the Ar^+ -Ar collision system, independent x-ray emission cross section determinations have been made.^{20,21} These agree within experimental error with the measurements presented in Fig. 2.

IV. DISCUSSION OF RESULTS

The structure observed in Fig. 2 for the Ar^+ -Ar x-ray emission cross sections σ_x at energies larger than about 30 keV is markedly at variance with the behavior of the total cross section for L -shell excitation in Ar^+ -Ar collisions as a function of energy. The total cross section

$$\sigma_T = \sigma_x + \sigma_A \quad (4)$$

is dominated by the Auger emission cross section σ_A , and these latter have been measured^{12,22} for incident energies up to 600 keV. σ_A shows a rapid rise in the neighborhood of 10 keV, then becomes essentially a constant function of energy from about

30 to 600 keV. The present results thus show that above about 30 keV, all the structure in σ_x is due to changes in the mean fluorescence yield $\bar{\omega}$ defined as

$$\bar{\omega} = \sigma_x / \sigma_T. \quad (5)$$

Thus, this structure is not due to changes in the L -shell excitation mechanisms, but instead is attributable to changes in the relaxation processes after vacancy creation. The total x-ray cross sections for Cl^+ -Ar collisions appear to follow similar behavior.

To understand this behavior, we need to examine the excitation mechanisms. Figure 3 schematically shows the correlation diagrams for the Ar-Ar and Cl-Ar molecules as functions of internuclear separation. As is well known,⁴⁻⁶ the excitation of the argon L shell in Ar-Ar collisions is due to promotion of electrons out of the $4f\sigma$ orbital during the collision. Because of the rapid rise of this orbital, and the many crossings it undergoes, this promotion is characterized^{5,12} by essentially unit probability of vacating both electrons occupying it for collisions in which the distance of closest approach is less than that associated with the rise. As discussed earlier,^{5,11,12} this leads to cross sections which rise rapidly at some threshold energy (the energy required for the atoms to reach the appropriate distance of closest approach — in this case about 8 keV), and become constant shortly thereafter. Additional L -shell promotions in the Ar-Ar system are possible via the $3d\sigma$ - $3d\pi$ - $3d\delta$ orbitals. These will be discussed later.

In the Cl^+ -Ar collisions, we see that the excitation of the chlorine L shell is also due to the $4f\sigma$ orbital, so that the behavior of the chlorine vacancy production cross section in Cl^+ -Ar collisions should be similar to that for Ar-Ar collisions. There is a difference in these cases, however. In Ar-Ar collisions, the two vacancies are shared by the two argon atoms. In Cl^+ -Ar collisions, both vacancies accrue primarily to the chlorine atom. This has been experimentally verified.^{5,10} In the Cl^+ -Ar collisions, additional vacancies in the chlorine L shell can occur via the $3d\pi$ - $3d\delta$ couplings, while argon L -shell vacancies can occur via $3d\sigma$ - $3d\pi$ - $3d\delta$ couplings.

The $4f\sigma$ and $3d\sigma$, $3d\pi$ promotions are very different in character. The latter two involve rotational couplings, with the near degeneracy of the orbitals occurring at zero internuclear separation. Explicit calculations of the $3d\sigma$ - $3d\pi$ - $3d\delta$ couplings¹³ show that the excitation probabilities are non-negligible only for distances of closest approach much smaller than those associated with the rise of the $4f\sigma$ orbital (i.e., of the order of 0.1–0.2 a.u.).

TABLE I. Mean fluorescence yields for Cl-Ar ($\sigma_I=4.35 \times 10^{-17} \text{ cm}^2$) and Ar-Ar ($\sigma_I=3.83 \times 10^{-17} \text{ cm}^2$) collisions.

E (keV)	$\bar{\omega}_L$ (Cl)	$\bar{\omega}_L$ (Ar)
50	6.2×10^{-3}	1.9×10^{-3}
100	2.2×10^{-2}	3.5×10^{-3}
200	4.6×10^{-2}	1.5×10^{-2}
500	5.2×10^{-2}	6.9×10^{-2}
1000	9.7×10^{-2}	7.3×10^{-2}
1500	1.03×10^{-1}	8.4×10^{-2}

Thus, the effect of the $3d$ promotions on the total vacancy production cross sections in either Ar⁺-Ar or Cl⁺-Ar collisions will be small compared to that of the $4f\sigma$ promotions and the total cross section will be dominated by the $4f\sigma$ promotion behavior.

As mentioned above in Cl⁺-Ar collisions the excitation of the argon L shell proceeds via the $3d$ orbital couplings. Thus this cross section should follow this rotational coupling behavior¹³ and have an effective threshold which is higher in energy. The results in Fig. 2 for $\sigma_x(\text{Ar})$ in Cl⁺-Ar collisions show this difference. Knowledge of the total excitation cross sections permits us to extract the mean fluorescence yields [Eq. (5)] as a function of bombarding energy. These are shown in Table I. The total cross sections for Ar⁺-Ar collisions were taken from Refs. 12 and 22 and extrapolated according to the above discussion. For Cl⁺-Ar collisions, the total cross sections were found using the data in Ref. 10 (see Ref. 11) and were also extrapolated.

Because we were unable to examine x rays above 284 eV photon energy we cannot perform an analysis of expected fluorescence yields as in Refs. 11 and 14. These additional x rays, though they contribute very little to the total x-ray cross sections, are important in correctly averaging the individual state contributions. However, the structure in σ_x can be qualitatively understood on the basis of the above discussion. The rapid rise in the mean fluorescence yield at about 150 keV reflects the effective onset of the $3d$ rotational couplings. This coupling produces additional vacancies in the respective L shells. When these multiple vacancies decay down to single vacancies via the Auger process, which is dominant, the resultant single

vacancy configurations have large numbers of M -shell vacancies, therefore much larger fluorescence yields.¹⁴ Note that the rise in the mean fluorescence yield tracks quite well the excitation of the argon atoms in Cl⁺-Ar collisions which occurs via rotational coupling. The decrease of the rate of rise at higher energies is most likely due to decrease in the Auger emission probability because the M -shell populations have been nearly depleted and the Auger rate depends on the number of electron pairs in the M shell. This effect is of course enhanced by the continued increase in direct M -shell excitation as a function of energy.

It may seem puzzling that, on the one hand, we state that the $3d$ promotions will contribute only little to the total excitation cross sections, and, on the other hand, that they are responsible for the rapid rise in σ_x . It must be remembered, however that the loss of two M -shell electrons increases the fluorescence yield by a large factor¹⁴; this increase more than compensates for the smallness of the $3d$ cross sections.

This discussion opens a number of avenues for further investigation. First, the total Auger cross sections at energies above 600 keV for Ar⁺-Ar collisions and at energies above 50 keV for Cl⁺-Ar collisions should be measured to verify their constancy. Second, Auger spectra should be measured for these collisions to gain some information on the nature of the resulting excited states. Third, the x-ray spectral measurements should be extended to photon energies greater than 284 eV. Fourth, evidence for multiple L -shell vacancies should be carefully examined as a function of energy. This information should help make a quantitative analysis of the excitation and relaxation mechanisms possible.

V. CONCLUSIONS

The total x-ray emission cross sections reported in this paper for Ar⁺-Ar and Cl⁺-Ar collisions for incident energies between 200 and 1500 keV show rapid rises in this energy range. These rises are compared to the behavior of the total vacancy production cross sections permitting extraction of the mean fluorescence yields as functions of energy. A qualitative explanation for these rises is given in terms of the L -shell promotion mechanisms in the quasimolecule formed by the collision partners.

¹V. V. Afrosimov, Y. S. Gordeev, M. N. Panov, and N. V. Fedorenko, Zh. Tekh. Fiz. 34, 1613 (1964) [Sov. Phys.-Tech. Phys. 9, 1248 (1965)].

²E. Everhart, and Q. C. Kessel, Phys. Rev. Lett. 14,

247 (1965).

³U. Fano and W. Lichten, Phys. Rev. Lett. 14, 627 (1965); W. Lichten, Phys. Rev. 164, 131 (1967).

⁴M. Barat and W. Lichten, Phys. Rev. A 6, 211 (1972).

- ⁵J. D. Garcia, R. J. Fortner, and T. M. Kavanagh, *Rev. Mod. Phys.* 45, 111 (1973).
- ⁶Q. C. Kessel and B. Fastrup, *Case Studies At. Phys.* 3, 137 (1973).
- ⁷J. S. Briggs and J. Macek, *J. Phys. B* 5, 579 (1972).
- ⁸J. S. Briggs and K. Taulbjerg, in *Topics in Modern Physics*, edited by I. Sellin (Springer, Berlin, to be published).
- ⁹F. W. Saris and D. Onderdelinden, *Physica (Utr.)* 49, 441 (1970); F. W. Saris, *ibid.* 52, 290 (1971).
- ¹⁰B. Fastrup, G. Hermann, and K. J. Smith, *Phys. Rev. A* 8, 1591 (1971).
- ¹¹R. J. Fortner, *Phys. Rev. A* 10, 2218 (1974).
- ¹²R. K. Cacak, Q. C. Kessel, and M. E. Rudd, *Phys. Rev. A* 2, 1327 (1970).
- ¹³G. B. Schmid and J. D. Garcia, *Phys. Rev. A* 15, 85 (1977).
- ¹⁴M. Chen and B. Crasemann, *Phys. Rev. A* 10, 2232 (1974).
- ¹⁵B. L. Henke, *Adv. X-Ray Anal.* I, 460 (1963).
- ¹⁶M. A. Spivack, *Rev. Sci. Instrum.* 41, 1614 (1970).
- ¹⁷R. J. Fortner and H. Oona, *Phys. Lett. A* 47, 276 (1974).
- ¹⁸R. J. Fortner, D. L. Mathews, and J. H. Scofield, *Phys. Lett. A* 53, 336 (1975).
- ¹⁹R. Kelly and L. Palumbo, NRL Report No. 7599, Naval Res. Lab., Washington, D.C. (1973) (unpublished).
- ²⁰H. Tawara, C. Foster, and F. J. DeHeer, *Phys. Lett. A* 43, 226 (1973).
- ²¹K. H. Schartner, H. Shaefer, and R. Hippler, *J. Phys. B* 7, L111 (1974).
- ²²N. Stolterfoht (private communication).